AD-A088 231 MCDONNELL DOUGLAS RESEARCH LABS ST LOUIS MO F/G 21/5
UNSTEADY TRANSONIC FLOWS IN A TWO-DIMENSIONAL DIFFUSER.(U)
MAY 80 M SAJBEN, T J BOGAR, J C KROUTIL F49620-77-C-0082
UNCLASSIFIED AFOSR-TR-80-0628 NL

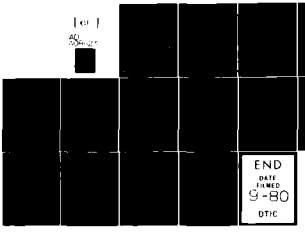

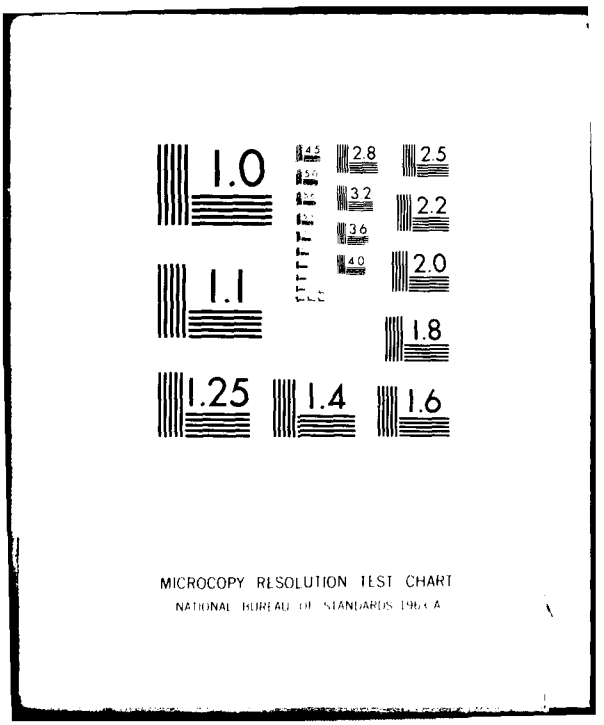
1.0
1.1
1.25
1.4
1.6
1.8
2.0
2.2
2.5
2.8
3.2
3.6
4.0
4.5
5.0
MICROCOPY RESOLUTION TEST CHART
NATIONAL BUREAU OF STANDARDS 1963 A

UNCLASSIFIED

SECURITY CLASSIFICATION OF THIS PAGE (When Data Entered)

REPORT DOCUMENTATION PAGE

READ INSTRUCTIONS BEFORE COMPLETING FORM

1. REPORT NUMBER: AFOSR-TR-80-0628
2. GOVT ACCESSION NO.: AD-A088 231
3. RECIPIENT'S CATALOG NUMBER:

4. TITLE (and Subtitle): UNSTEADY TRANSONIC FLOWS IN A TWO-DIMENSIONAL DIFFUSER

5. TYPE OF REPORT & PERIOD COVERED: Annual Rept. 1 Apr 79 — 31 Mar 80

6. PERFORMING ORG. REPORT NUMBER:

7. AUTHOR(s): M. SAJBEN, T. J. BOGAR, J. C. KROUTIL

8. CONTRACT OR GRANT NUMBER(s): F49620-77-C-0082

9. PERFORMING ORGANIZATION NAME AND ADDRESS:
MCDONNELL DOUGLAS RESEARCH LABORATORIES
MCDONNELL DOUGLAS CORPORATION
ST. LOUIS, MO 63166

10. PROGRAM ELEMENT, PROJECT, TASK AREA & WORK UNIT NUMBERS: 2307A4, 61102F, A4

11. CONTROLLING OFFICE NAME AND ADDRESS:
AIR FORCE OFFICE OF SCIENTIFIC RESEARCH/NA
BLDG. 410
BOLLING AIR FORCE BASE, D.C. 20332

12. REPORT DATE: May 1980

13. NUMBER OF PAGES: 27

14. MONITORING AGENCY NAME & ADDRESS (if different from Controlling Office)

15. SECURITY CLASS. (of this report): UNCLASSIFIED

15a. DECLASSIFICATION DOWNGRADING SCHEDULE

16. DISTRIBUTION STATEMENT (of this Report)

Approved for public release, distribution unlimited.

17. DISTRIBUTION STATEMENT (of the abstract entered in Block 20, if different from Report)

18. SUPPLEMENTARY NOTES

19. KEY WORDS (Continue on reverse side if necessary and identify by block number)

TRANSONIC FLOW
FLOWFIELD OSCILLATIONS
TWO-DIMENSIONAL MODEL
AIR BREATHING PROPULSION SYSTEMS

20. ABSTRACT (Continue on reverse side if necessary and identify by block number)

Extensive measurements of shock position and pressure distributions (wall static, core flow static, and core flow total) were made, complemented by spark schlieren and high-speed schlieren photographic information. Measurements were made at shock Mach numbers up to 1.35, with and without excitation. The excitation amplitudes were low, with frequencies from 0 to 330 Hz.

DD FORM 1 JAN 73 1473

UNCLASSIFIED

SECURITY CLASSIFICATION OF THIS PAGE (When Data Entered)

20. ABSTRACT (Continued)

Unexcited flows displayed two dominant natural frequencies for attached flows (shock Mach numbers below 1.27) and one dominant peak for separated flows (shock Mach numbers above 1.28). The dominant frequencies depend strongly on shock strength.

Diffuser response to excitation appears to follow patterns expected on the basis of low-amplitude (acoustic) wave propagation concepts, provided that the stream-wise variation of the flow speed is considered and realistic boundary conditions are applied at the ends of the channel. Weak shocks produce weak reflections of arriving waves, but acoustic impedance increases sharply with shock strength, and shocks over M = 1.28 reflect waves with almost no attenuation. The presence of counter-running wave trains of comparable amplitude was illustrated by the presence of nodes in the periodic component of the static pressure distribution, detected at high Mach numbers and frequencies above 200 Hz.

The study strongly suggests that the effective acoustic impedance associated with the shock/boundary-layer interaction zone is an important determinant of diffuser response to small-amplitude external perturbations.

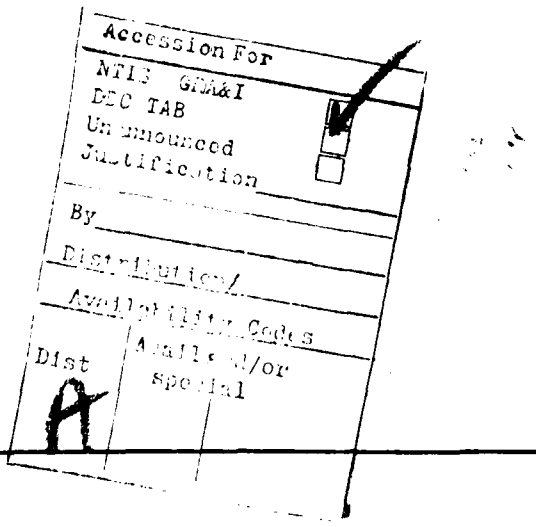

1. INTRODUCTION

F49620-77-C-0082

This report describes the results obtained in the third year of a continuing investigation of unsteady, transonic flows, with applications to dynamic distortion in inlets of jet aircraft and to pressure oscillations in ramjet propulsion systems.[1-3]

The first year of the contract was devoted to exploring the effects of approach boundary-layer thickness on the dynamic behavior of a two-dimensional diffuser with an area ratio of 2.37. The diffuser displayed intense, self-excited fluctuations whose properties were studied in detail.[4,5]

The second and third years constitute the second phase. The goal of this phase is to explore the response of a diffuser of area ratio 1.5 to periodic perturbations imposed at the downstream end. This experiment is related to the problem of ramjet inlet response to pressure fluctuations caused by combustion instabilities in the combustor. The results also serve as benchmark data for validating related theoretical approaches, including one in progress at MDRL.

Experimental work and data reduction for the second phase are complete; detailed documentation is under preparation.

2. RESEARCH OBJECTIVES

The specific objectives of the second phase are as follows:

1) Design and build appropriate hardware suitable for creating nearly planar, periodic waves downstream of the diffuser model.

2) Obtain detailed steady and dynamic measurements of the surface pressures and shock positions at various pressure ratios and perturbation parameters.

3) Obtain phase-averaged flowfield velocity and velocity fluctuation measurements at selected test parameter combinations.

4) Reduce, analyze, and document data in a form useful for comparison with theoretical prediction methods.

3. EXPERIMENTAL EQUIPMENT

3.1 Diffuser Model

The diffuser model used (Figure 1) was available from a related, MDRL-sponsored experimental effort. The model is a third-generation design and incorporates the experience from three years of related work. The exit-to-throat area ratio is 1.52, the ratio of divergent length to throat height is 7.2, and the aspect ratio of the throat cross-section is 4. The throat height is 44 mm. Sidewall and bottom boundary-layer growth is limited by three sets of ram-type suction slots, with independently controlled and measured flow rates. The sidewalls are 2.54-cm-thick, schlieren-quality glass panels.

The model is supplied with clean, dry air through a plenum chamber equipped with a 25:1 area ratio contraction section. The air exhausts to the laboratory, keeping the exit pressure constant. Shock strength is varied by controlling the plenum chamber pressure and thereby the overall pressure ratio (ratio of plenum total to exit static pressures). The shock strength increases monotonically with pressure ratio; the strongest obtainable shock Mach number is $M_\sigma \approx 1.35$.

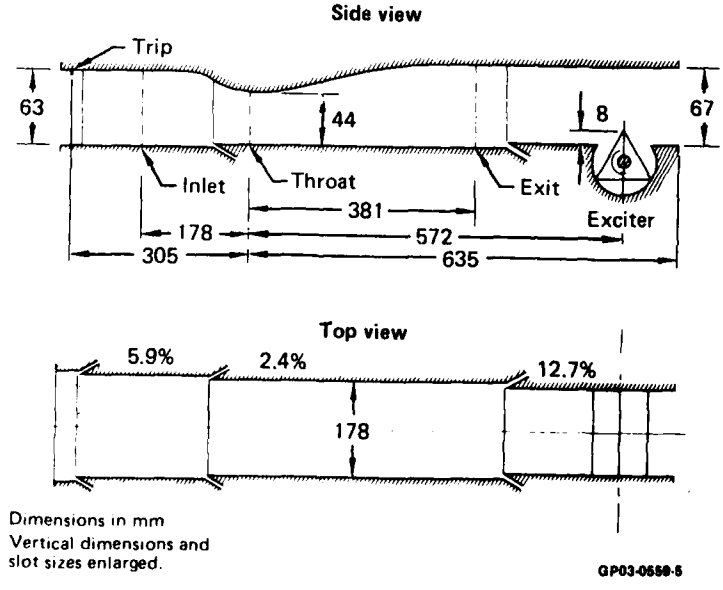

Figure 1. Diffuser model. Exit-to-throat area ratio = 1.5, aspect ratio of throat cross section = 4.0. Percentages given near each slot indicate slot area as a fraction of cross section area immediately upstream of slot.

3.2 Perturbation Generator

The perturbation of the time-mean flow was accomplished by mechanical modulation of the exit cross-sectional area. The active element of the modulating device was a triangular, prism-shaped rotor revolving around a spanwise axis, driven by a variable-speed motor (Figure 2). Oscillation frequencies could be continuously varied from 15 to 330 Hz, and rotor immersion could be adjusted stepwise from 0 to 13 mm.

An optical encoder, mounted on the rotor shaft, produced one pulse per revolution (one pulse per three oscillation cycles), which was used in the data reduction process as a synchronous signal to initiate sampling and averaging operations.

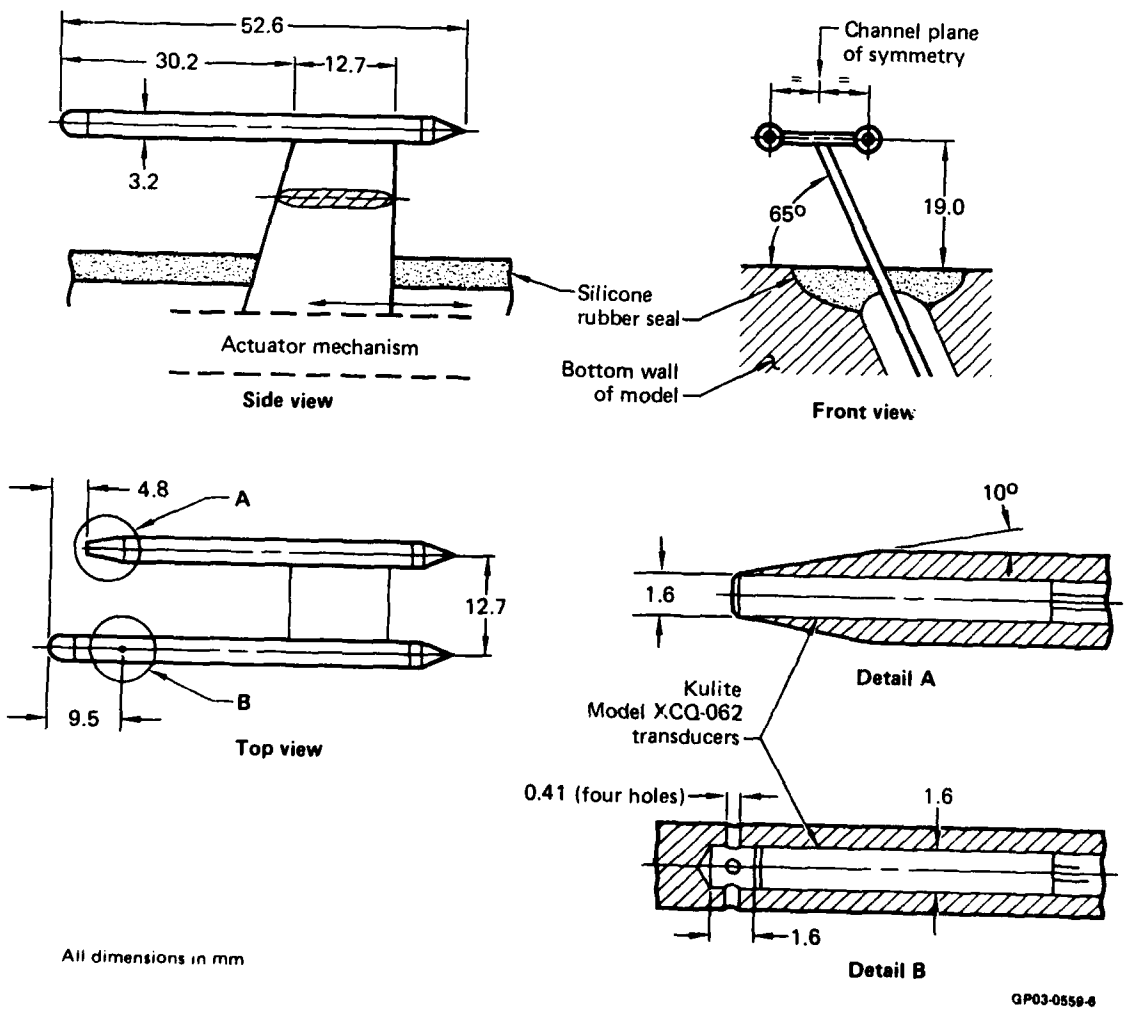

Figure 2. Core flow probe.

3.3 Instrumentation

A total of 15 time-mean flow properties were routinely monitored and recorded throughout the test series, including pressures, temperatures, primary flow rate, individual bleed flow rates through each slot, mean and rms values of shock position, and mean and rms values of surface pressure fluctuations at selected locations. Time-mean wall pressure distributions were determined by numerous wall static orifices for all operating conditions of significance, using a 96-channel Scanivalve system.

Fluctuating wall surface pressures were measured by high-response transducers at seven streamwise positions on the top wall. One of these stations, the exit, is an important reference location and was equipped with four transducers, two on the top wall and two on the bottom wall.

Two diagnostic methods were of particular importance to this study. An optical technique was used to generate an instantaneous shock-position signal which was of central significance among the measured quantities. The system, developed at MDRL, used a line-scan, imaging camera incorporated into the schlieren system of the facility and complemented with appropriate electronic signal processing equipment. A detailed description of this system[7] is available. The second method used a dual pressure probe to detect instantaneous total and static pressures within the core flow. The probe (Figure 2) was mounted in a traverse gear embedded in the lower diffuser wall to allow the probe to be positioned in the streamwise direction from $\tilde{x} = 0$ to 8. The sensing elements were miniature pressure transducers with an (unmounted) natural frequency of 500 kHz. The probe did not cause appreciable alteration in the wall static pressure distributions, nor have an influence on the overall integral performance parameters (such as mass flow ratio or pressure recovery) unless it was located sufficiently close to the shock to pierce it intermittently.

All dynamic data were recorded on FM tape, using a 14-channel (Sangamo Sabre III) tape recorder.

4. TEST RESULTS

The experimental program was completed, and the data were reduced and machine-plotted in a format acceptable for data reports. The collection of data is voluminous even in this condensed, graphic representation, and only an overview is given here.

The time-mean behavior of the investigated model was discussed in the previous Annual Report.[6] Subsequent paragraphs deal only with the unsteady properties of the flow. Appendix A defines the nomenclature used in this Report.

4.1 Unexcited Flow

The diffuser flow exhibited unsteady fluctuations at all shock Mach numbers. The amplitudes of pressure and shock displacement were small compared with earlier diffuser experiments involving the (higher) area ratio range from 1.842 to 2.5.[1-3,5] This behavior was consistent with the observation that in the present model the boundary layers were attached everywhere up to M = 1.27 and tha the separation bubble (which did exist at higher Mach numbers) was at most six throat heights long. In earlier experiments, the top-wall boundary layer was separated under all conditions, and the separation bubble length varied from 6 to 12 throat heights.

Test parameters and the type of data available for each test condition are summarized in Table 1.

TABLE 1. TIME-DEPENDENT DATA RECORDS AVAILABLE FOR UNEXCITED FLOWS.

$M_{\sigma u}$	Data type			$M_{\sigma u}$	Data type		
	σ*	u+	m†		σ	u	m
1.153	x	x		1.274	x	x	
1.173	x	x		1.276	x	x	
1.229	x	x	x	1.278	x	x	x
1.244	x	x		1.286	x	x	
1.258	x	x		1.292	x	x	
1.263	x	x		1.302	x	x	
1.266	x	x		1.312	x	x	
1.268	x	x		1.344	x	x	x
1.270	x	x					

* Shock position from line-scan system

\+ Upper wall static pressures at 7 positions: $\bar{x}$ = 2.43, 3.13, 4.61, 6.37, 8.65, 10.95, and 14.12

† Core flow probe static and total pressures $\bar{y}$ = 0.432, $\bar{x}_\sigma < \bar{x} \leq 8.05$, at 16 locations

GP03-0559-3

4.1.1 Shock Motion

The shock motion is governed by the static pressure variation at the downstream side of the shock, corresponding to the overall, longitudinal oscillation pattern existing in the duct. The shock is thus a sensitive indicator of the amplitudes and frequencies associated with the large-scale fluctuations, and its motion is perhaps the most significant information obtained in this phase of the study.

The rms values of the shock displacement are shown in Figure 3. The magnitudes are small; even peak-to-peak values are at most 20% of the throat height. The flow is fully attached up to $M_{\sigma u} = 1.266$ and is fully separated beyond $M_{\sigma u} = 1.276$. The attached and separated flows display different characters; variation is modest for attached flow, but amplitudes rise steeply when the flow is separated. The transition between the two types of flow occurred intermittently: the flow alternated randomly between the two modes at frequencies that were sufficiently low to be observed visually (0.5-3 Hz).

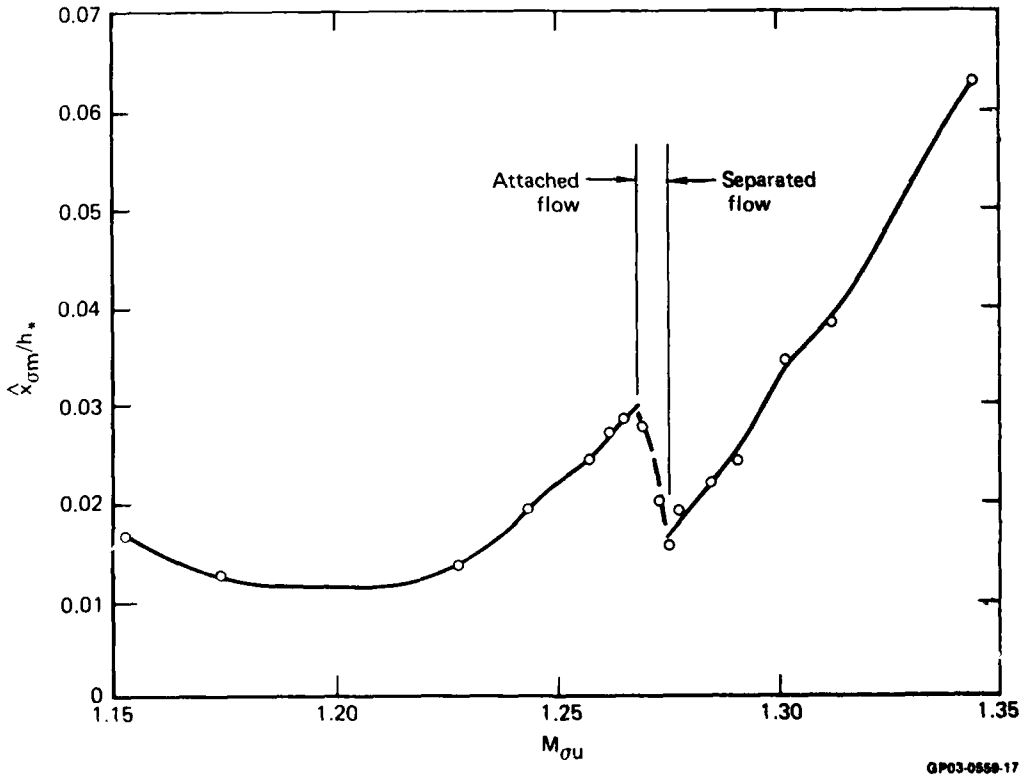

Figure 3. Shock displacement rms values.

The power spectral density distributions for $\tilde{x}_{\sigma m}$ have a bimodal shape for attached flows and display a single dominant frequency for separated flows (Figure 4). The frequencies associated with the spectral peaks are summarized as functions of the shock Mach number, $M_{\sigma u}$, in Figure 5.

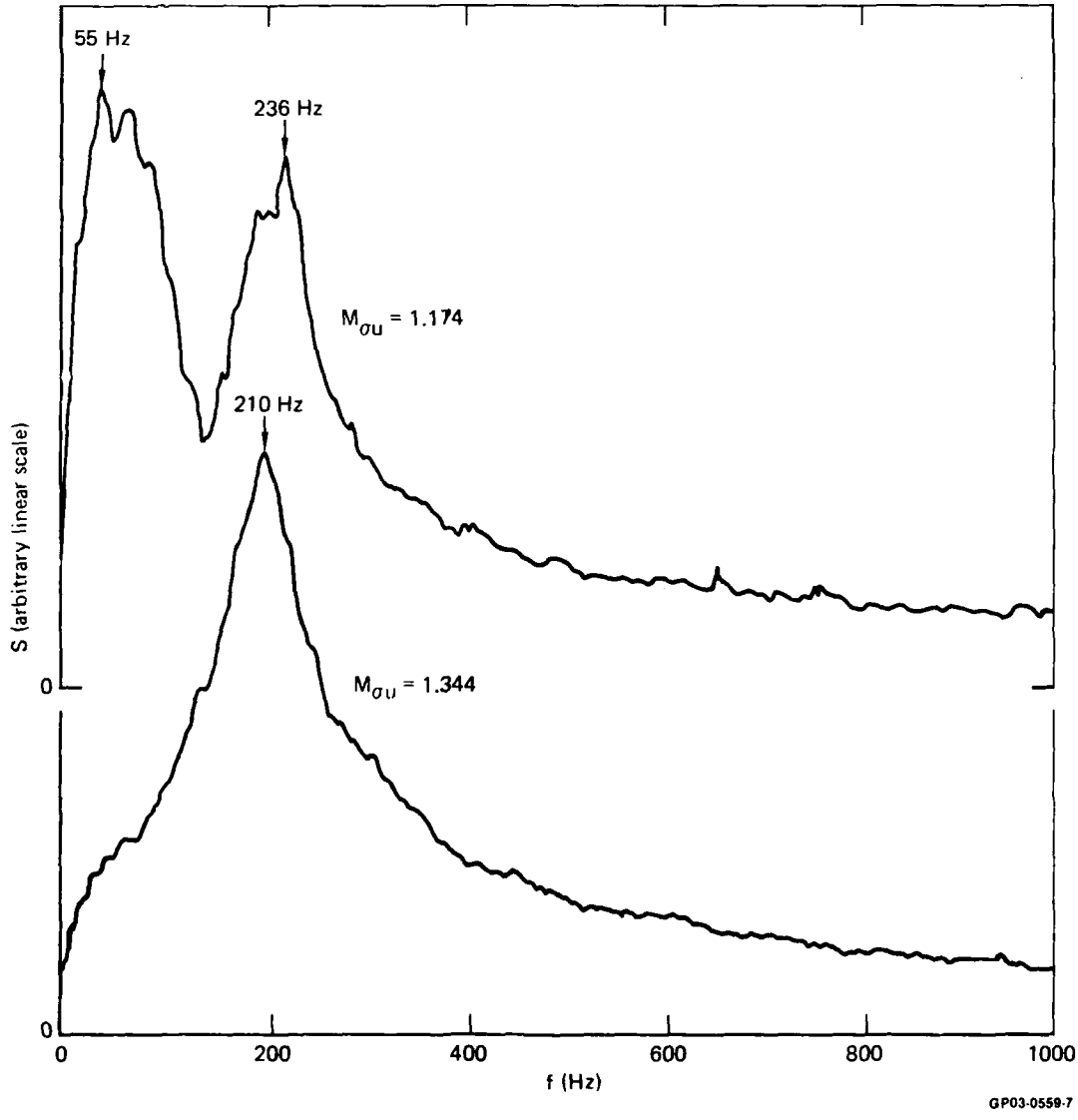

Figure 4. Power spectral density distributions for shock displacement at two selected shock Mach numbers.

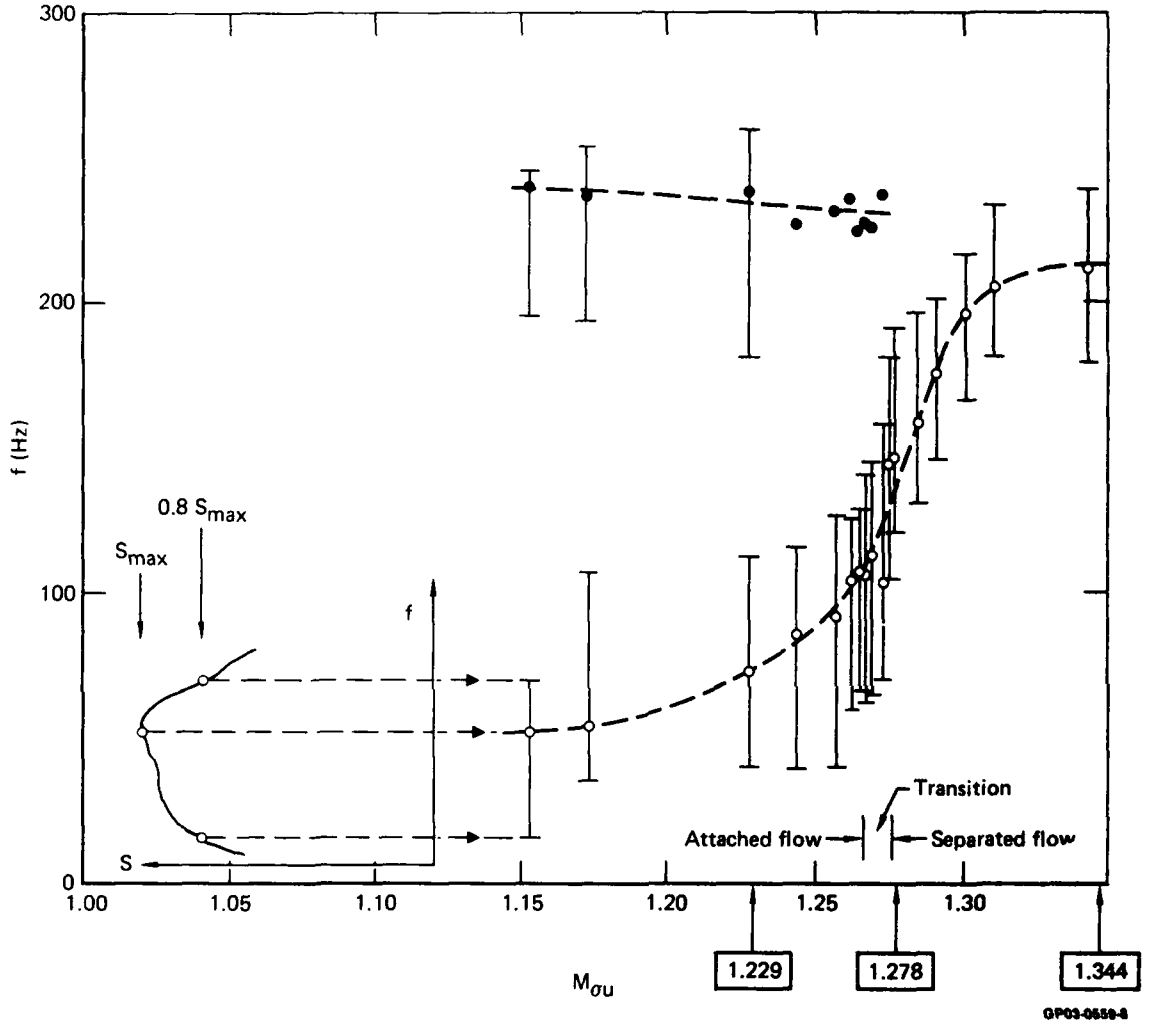

Figure 5. Peak frequencies from shock displacement spectra. Insert at left indicates how error bars designate width of spectral peak. Framed numbers below horizontal axis designate conditions selected for detailed study with excitation.

The high-frequency peak is reasonably independent of $M_{\sigma_{11}}$, but the low-frequency peak varies greatly from approximately 50 Hz to 210 Hz. Most of the increase occurs near M = 1.275 where separation begins. The wide range and the continuous variation of the natural frequencies are difficult to interpret in terms of simple acoustic modes since neither geometric lengths nor wave speeds vary greatly over the test conditions.

One may speculate that the natural frequencies are strongly influenced by the length of the inviscid core flow (the length between the shock and the location where the two wall boundary layers merge) since this length varies considerably. A second possible factor responsible for the wide variations could be the character of the reflection of waves at the shock (i.e., the acoustic impedance). The reflection here is influenced not only by the shock wave, but also by the area changes associated with local, rapid variations of the boundary-layer displacement thickness. Since the character of the shock/boundary-layer interaction changes considerably over the Mach number range tested, it is reasonable to expect that the acoustic impedance varies also. The wavelength/geometric-length ratios depend strongly on the boundary conditions, and thus the variation of natural frequencies may be related to parallel changes in the properties of the interaction region.

4.1.2 Pressure Distributions

The intensities of static and total pressure fluctuations sensed by the core flow probe are illustrated in Figure 6. The static pressure fluctuations are uniform over the length of the model, but increase considerably with shock strength, as expected. The total pressure fluctuations behave in the opposite way: they increase sharply with $\tilde{x}$ but do not depend strongly on $M_{\sigma u}$. The time-mean total pressure is nearly constant over the $\tilde{x}$ range of Figure 6 and the core flow is essentially irrotational. The total pressure fluctuations, which primarily reflect velocity fluctuations, are thought to be irrotational movements induced by the large-scale turbulence at the boundary-layer/core-flow interface.

The power spectral density distributions for the core flow and wall pressure fluctuations indicate that most of the fluctuating energy resides at frequencies above 5 kHz and substantial contributions are made at frequencies above the experimental cutoff of 10 kHz. These high frequencies are associated with boundary-layer turbulence and not with the low-frequency acoustic motion characterized by the shock displacement spectra. The contribution from low frequencies to the overall pressure fluctuation is only a minute fraction of the total.

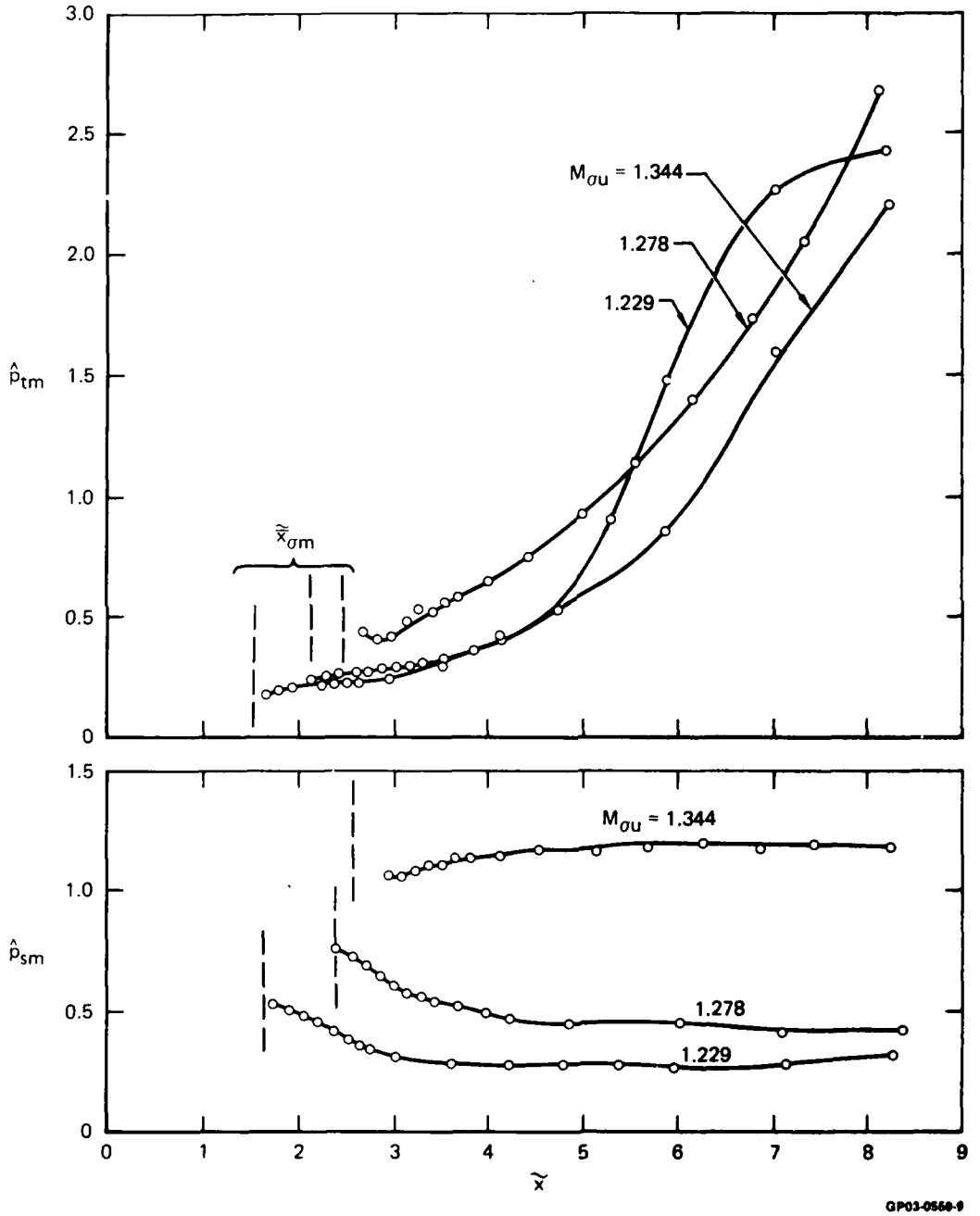

Figure 6. Total and static fluctuating core flow probe pressure rms distributions. Vertical dashed line segments indicate time-mean shock locations.

This observation is consistent with the explanation offered in Reference 5 for the existence of large-scale fluctuations. If the boundary-layer turbulence frequencies in some region within the diffuser decrease to the low values comparable to the longitudinal acoustic modes of the duct, then the latter are excited and intense fluctuations of the shock occur. These fluctuations then may feed back into the boundary layer, as was the case with the 2.37 area ratio model of Reference 5. In the present model, the core flow velocities are higher, and the boundary layers are thinner, attached, and display at most small separation bubbles. All these factors combine to produce high turbulence frequencies and minimal acoustic mode excitation. As a consequence of the small pressure amplitudes, the amplitudes of the shock motion are also small.

4.2 Excited Flow

The response of the diffuser to periodic variations of the exit pressure was investigated for three selected shock strengths corresponding to attached, transitional, and separated boundary layers. Figure 5 illustrates how these choices relate to the natural frequencies of the model. For certain selected frequencies, detailed streamwise surveys of mean and fluctuating core flow properties were made using the core flow probe. The selected frequencies lie either at, or far from, the natural frequencies of Figure 5 as an attempt to determine the existence of resonant behavior. The combinations of test parameters and the data taken are summarized in Table 2.

Eleven channels of dynamic data were recorded on FM tape simultaneously with reference pulses from the encoder mounted on the exciter shaft. The data were subsequently processed in the following manner:

The analog data were digitized at 20 kHz for a period corresponding to 150 oscillation cycles. The data for each individual cycle were then replaced by a set of 360 interpolated points, corresponding to constant phase angle increments of 1 deg, as opposed to a constant increment of time. This procedure compensated for any unsteadiness in exciter angular speed. The interpolated data were then averaged over 150 oscillation cycles, yielding an average waveform and the standard deviation of the 150 samples taken. The average of these standard deviations over the phase angles is a measure of the time-mean contribution of random processes to the signal, most of which is due to turbulence.

TABLE 2. TIME-DEPENDENT DATA RECORDS AVAILABLE FOR EXCITED FLOWS.

$M_{\sigma u}$ =	1.229			1.278			1.344		
f (Hz)	Data type			Data type			Data type		
	σ*	u*	m*	σ	u	m	σ	u	m
15	x	x		x	x				
30	x	x		x	x		x	x	
45	x	x		x	x				
60	x	x		x	x	x	x	x	
75	x	x	x	x	x		x	x	
90	x	x		x	x		x	x	
100							x	x	x
105	x	x		x	x		x	x	
120	x	x		x	x	x	x	x	
135	x	x		x	x		x	x	
150	x	x	x	x	x		x	x	
165	x	x		x	x		x	x	
180	x	x		x	x	x	x	x	
195	x	x		x	x		x	x	
200							x	x	x
210	x	x		x	x		x	x	
220	x	x	x						
225	x	x		x	x		x	x	
240	x	x		x	x		x	x	
250				x	x	x			
255	x	x		x	x		x	x	
270	x	x		x	x		x	x	
300	x	x	x	x	x	x	x	x	x
330	x	x		x	x		x	x	

*See Table 1 notes for definition

GP03-0550-4

The average waveforms were next Fourier analyzed to determine the amplitude and phase of the first four harmonic components. The fundamental or first harmonic was of most interest because it corresponds to the excitation frequency.

The excitation technique employed is such that the area perturbation has a nonzero mean value. This arrangement necessitated slight adjustments of the inlet pressure to obtain the same shock location and the same time-mean flow for each excitation frequency. The velocity distributions of Figure 7, obtained from core probe data, show that this adjustment accomplished the desired goal and that the mean flow properties are effectively constant for any given frequency sweep.

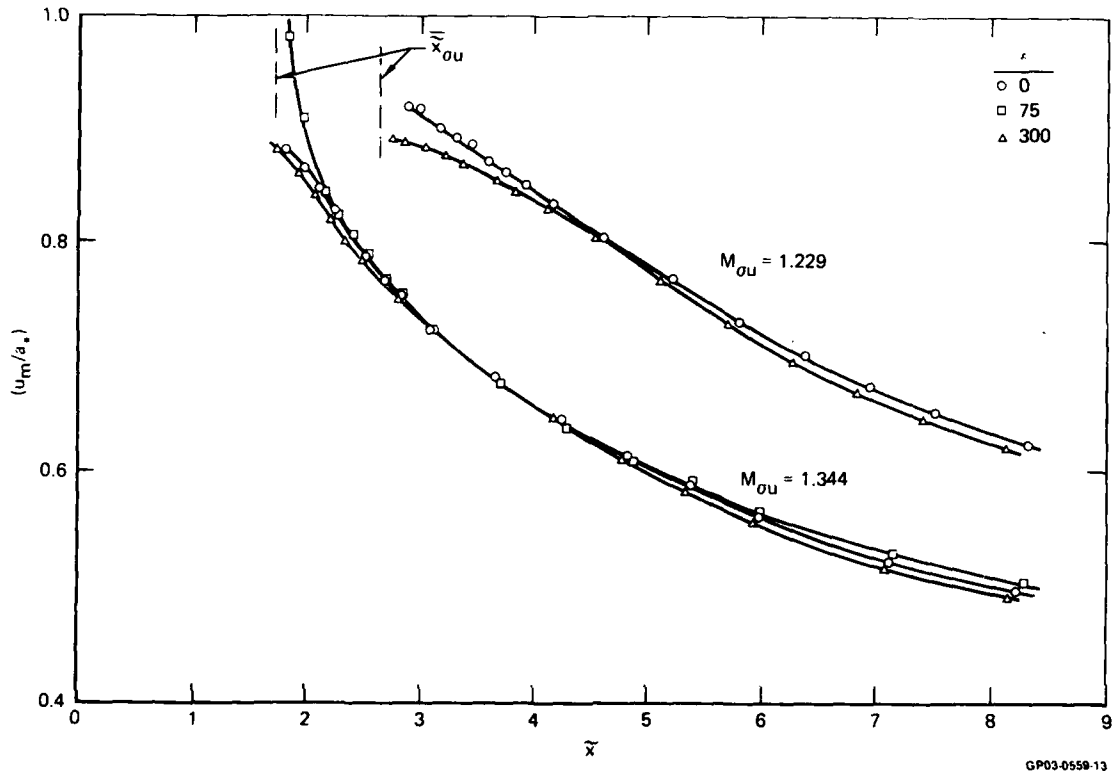

Figure 7. Streamwise distributions of core flow speed for different shock strengths and frequencies.

4.2.1 Exit Station Pressure

As mentioned earlier, the exit pressures serve as reference quantities characterizing the perturbation imposed on the flow, even though the perturbations are actually generated at the exciter located further downstream. The signals serve as the equivalent of burner pressure fluctuations (when relating the results to ramjet pressure fluctuations) or as boundary conditions (when using the data to verify relevant theoretical prediction methods).

The time history of wall static pressures was monitored carefully at the exit station ($\tilde{x}$ = 8.65) using two wall-mounted high-response transducers on the top and bottom walls. The signals showed a nearly sinusoidal shape (Figure 8) and displayed no detectable phase shifts, indicating the absence of spanwise or vertical misalignment of the wavefronts.

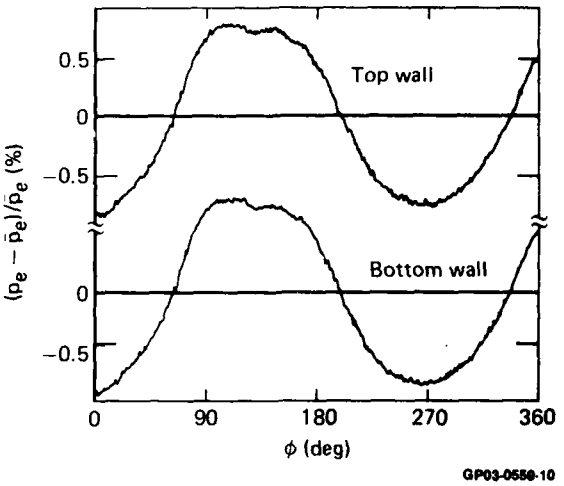

Figure 8. Signal-averaged wall pressure waveforms at the diffuser-exit station, $M_{\sigma u}$ = 1.235, f = 165 Hz. Lack of phase shift between top and bottom signals indicates planar wave-front.

Figures 9 and 10 illustrate the properties of the exit pressure fluctuations as they depend on excitation frequency, for attached and separated flow conditions, respectively. The rms intensities vary between 0.5 and 2.0% of the local static pressure and, therefore, are relatively small compared with fluctuations observed in ramjet burners, which may reach amplitudes of 10% or greater. On the other hand, the small amplitude increases the chances of successfully describing the observed phenomena with the aid of linearized theories.

Figures 9 and 10 clearly show that the contribution of higher harmonics is small compared with that of the first, which simplifies data interpretation. The amplitude of the first harmonic depends strongly on frequency in both cases. Attempts to vary amplitudes by changing the immersion depth of the rotor proved inadequate, and all data reported here correspond to the frequency/amplitude relations given in Figures 9 and 10 (rotor immersion depth = 6.4 mm).

Analysis of the data gave strong indications that the perturbations indeed behave as expected on the basis of linear theory, implying that amplitude effects are negligible, and normalization by the amplitude of the input perturbation is an acceptable procedure.

The magnitudes of the random contributions also are illustrated on Figures 9 and 10. The magnitude in each case is independent of the perturbation amplitude. For weak shocks, the perturbation amplitudes dominate, while in the case of a strong shock, the periodic and random components are the same magnitude. Despite the high noise level, the averaging and harmonic analysis procedures permitted the determination of important trends and relations, to be discussed in the following paragraphs.

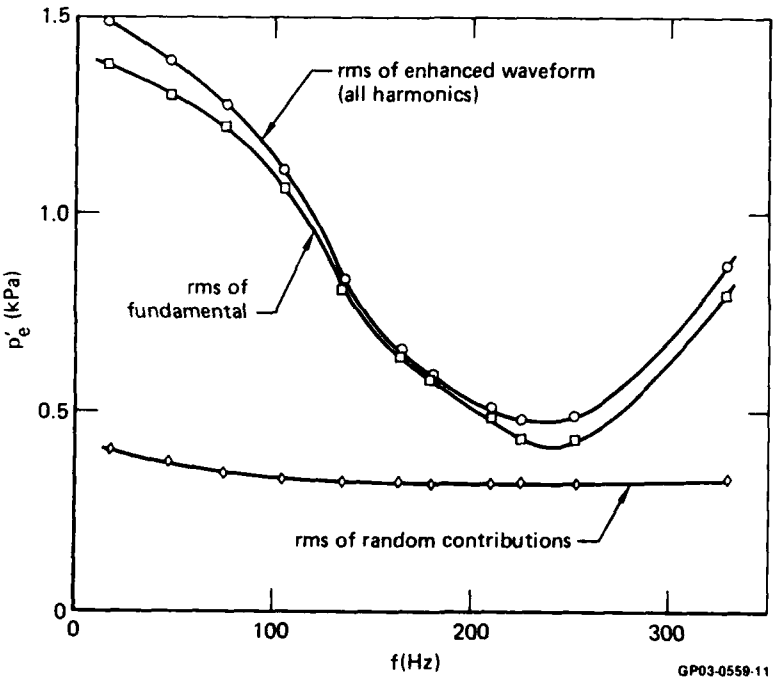

Figure 9. Exit wall static pressure perturbation amplitude vs frequency for $M_{\sigma u}$ = 1.229.

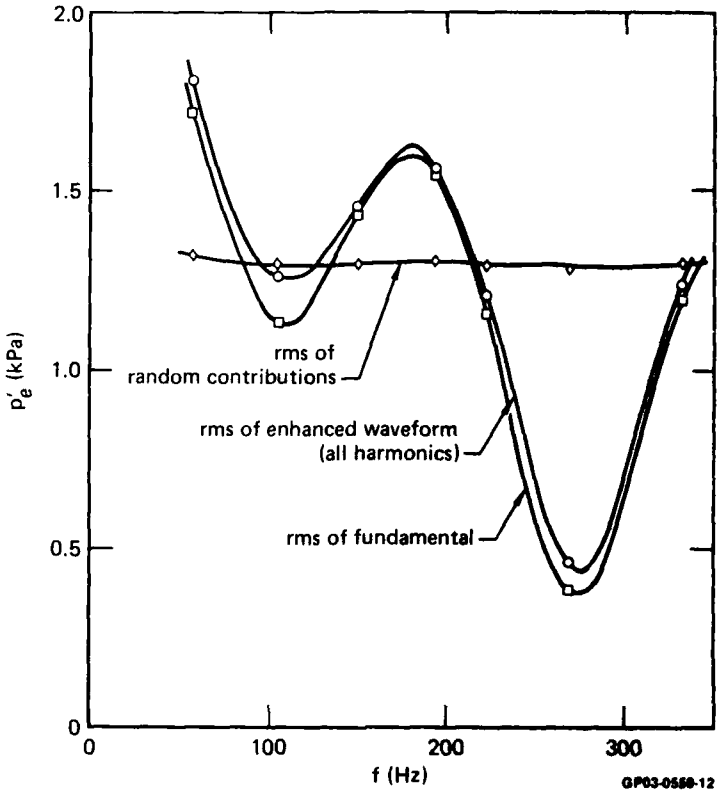

Figure 10. Exit wall static pressure perturbation amplitude vs frequency for M_{cu} = 1.344.

4.2.2 Weak Shocks (M = 1.229)

Figure 11 shows the shock displacement rms values as a function of frequency. The amplitudes follow the trends of the input pressure amplitudes and contain only small contributions from higher harmonics. The amplitudes are well above the unexcited fluctuation levels illustrated in Figure 3.

The most interesting feature of Figure 11 is the absence of resonant behavior near the natural frequencies of 75 and 220 Hz. Even if the shock amplitudes are normalized by the input amplitudes of Figure 9, the shock motion has a minimum amplitude of f = 220 Hz. One possible explanation for the absence of resonant behavior is that the natural mode is excited by the turbulent boundary layer in a distributed manner, involving much of the streamwise length of the diffuser. In contrast, the artificial excitation applied here is concentrated at one point near the duct end. The difference between the methods of excitation may cause different modes to be excited in the two cases.

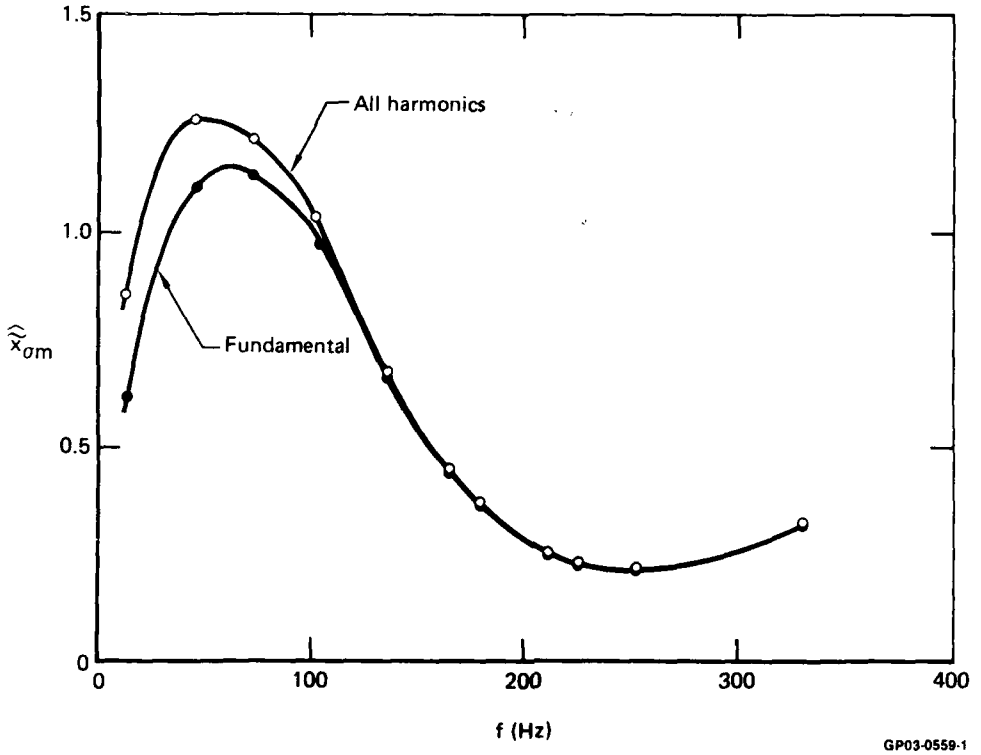

Figure 11. Shock displacement rms amplitudes for $M_{\sigma u}$ = 1.229.

Figure 12 shows x-t trajectories constructed from phase-angle information for the first harmonic, generated in the Fourier analysis. Each curve can be considered as the trajectory of a wave crest as it propagates upstream, and the slope of the curve represents the phase velocity of the particular wave.

The pattern shown in Figure 12 corresponds, in most but not all aspects, to the original expectations based on the following physical picture. Pressure waves generated by the exciter propagate upstream at the speed (phase velocity) of a - u. This speed varies along the diffuser from approximately 120 to 180 m/s. A weak normal shock is expected to produce a negligible reflection, and therefore the duct should contain only one family of waves, as in fact is observed in Figure 12. The phase velocity of the waves, however, seems to depend on the excitation frequency and attains unrealistically high values (230 m/s).

Analytical considerations of a simple one-dimensional model indicate that this tendency can be explained by assuming that the reflection from the shock is of small but significant amplitude. In this case the upstream and downstream running waves combine to form a resultant wave train that is also a traveling wave. The phase velocity of this resultant train depends on frequency with the qualitative trends as observed in the data.

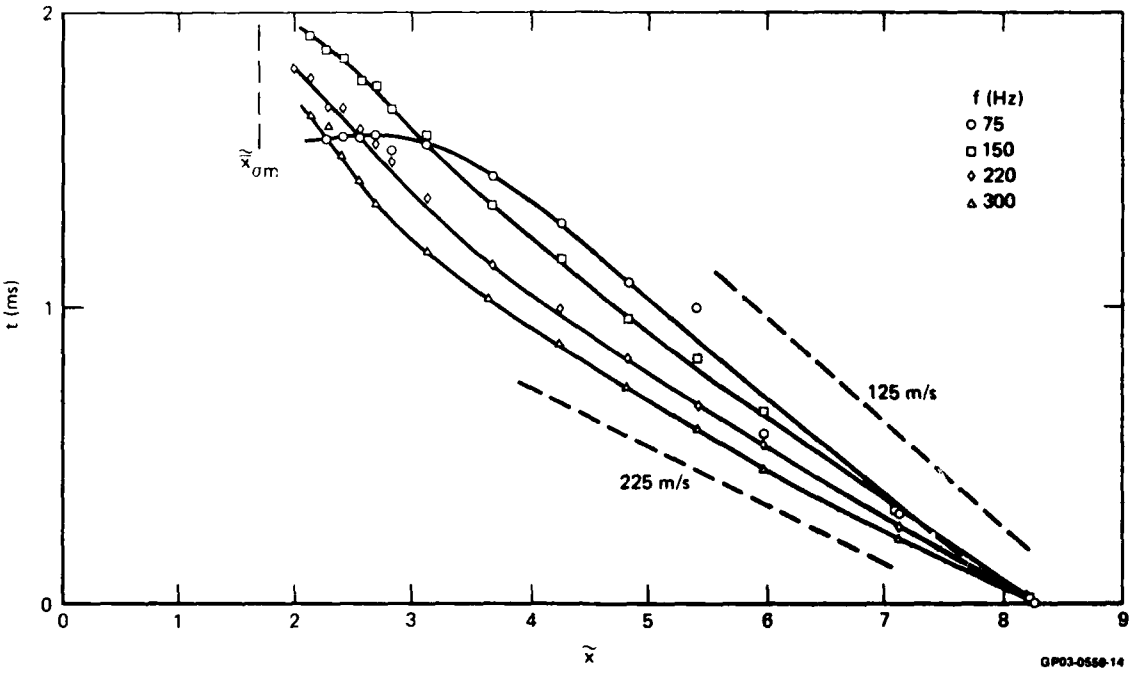

Figure 12. Wave trajectories from phase angle information for the first harmonic of the core flow probe static pressure signal, $M_{\sigma u} = 1.229$.

Figure 13 shows the amplitude of the fundamental mode of the core flow static pressure perturbation, normalized by the amplitude at $\tilde{x} = 8.25$, as a function of $\tilde{x}$. The perturbation amplitudes increase as the upstream moving waves encounter higher mean Mach numbers. The amplitude is more than doubled by the time the wave reaches the shock. As the excitation frequency increases, the amplification generally begins at a further upstream location. This behavior is consistent with the predictions of transonic, small-disturbance theory applied to diffusers (Reference 6).

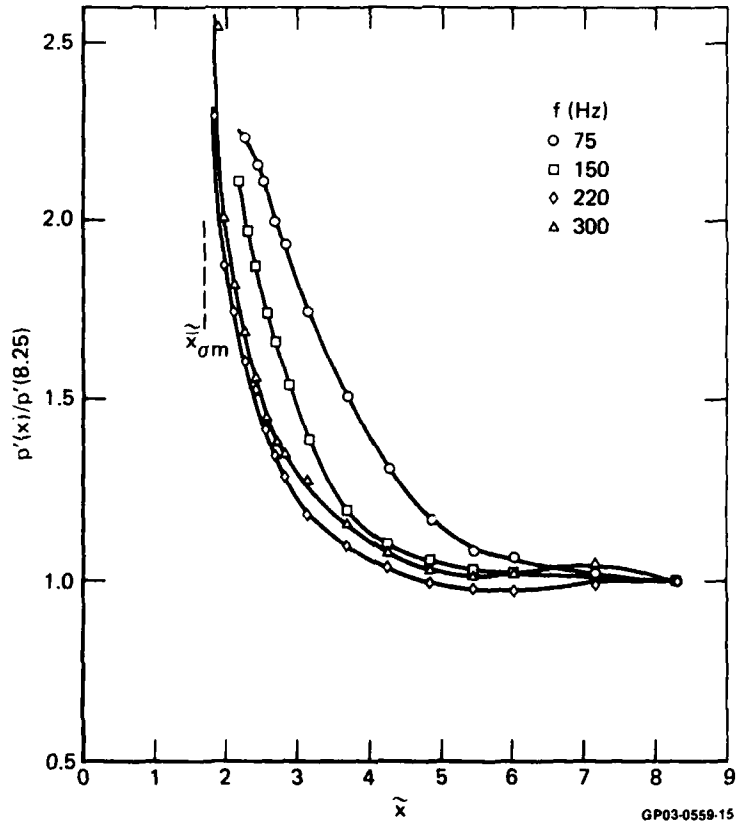

Figure 13. Amplitude distributions for the first harmonic of the core flow probe static pressure signal, $M_{\sigma u}$ = 1.229.

4.2.3 Strong Shock (M = 1.344)

Figure 14 illustrates the shock displacement amplitudes as a function of excitation frequency. The amplitudes are smaller than those detected for the weak shock case and do not vary greatly with frequency. The motion is nearly sinusoidal, with only a small higher harmonic content. As was the case with weak shocks, there is no significant evidence of resonant behavior near the natural frequency of 210 Hz.

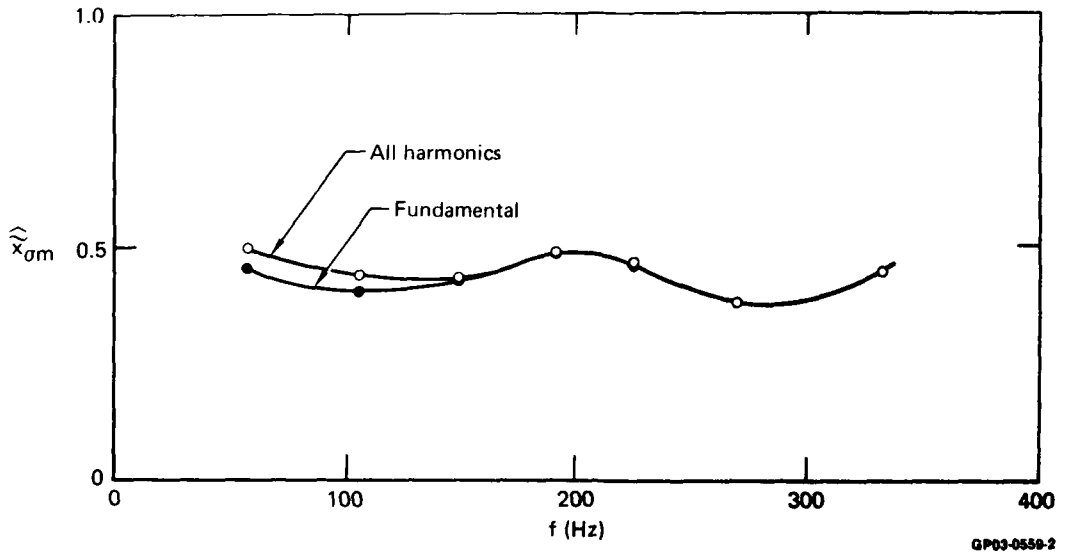

Figure 14. Shock displacement rms amplitudes for $M_{\sigma u} = 1.344$.

Figure 15 illustrates the streamwise amplitude and phase angle distributions of the core-flow static pressure perturbation for the fundamental mode at 300 Hz excitation frequency. The most striking feature of the plot is the presence of a nodal point, manifested by a location of zero amplitude and a concurrent 180° phase shift. There is also a strong suggestion that a second nodal point might exist near $\tilde{x} = 10$, beyond the range of the core probe traverse gear.

Nodal points cannot exist without the presence of two wave trains capable of canceling each other at any instant. The normal shock (or its immediate vicinity) must be therefore a strong reflector of incoming waves capable of producing a downstream-running wave train whose amplitude is nearly equal to the incident one. Since the amplitude is near its maximum at the shock, the reflection must occur in a like sense, i.e., an incoming compression wave produces a reflection that is also a compression wave (vice versa for expansion waves). This conclusion is consistent with an earlier conjecture based on surface pressure cross-correlation maps of unexcited diffuser flows (Reference 4).

The implied strong, closed-end type reflection at the shock cannot be explained by one-dimensional arguments based on the Rankine-Hugoniot relations. An analysis of the interaction between a stationary normal shock

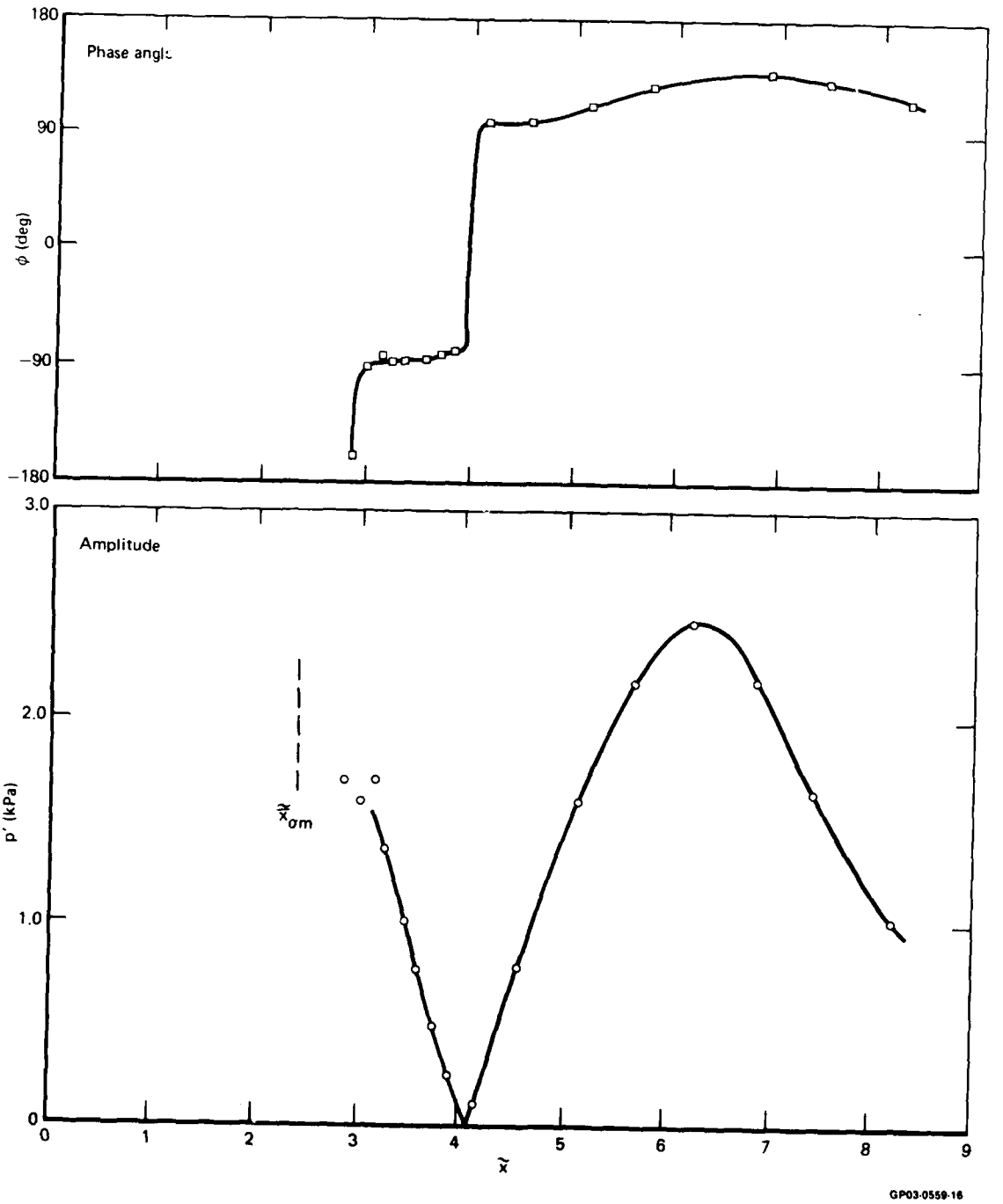

Figure 15. Phase angle and amplitude for the first harmonic of the core flow static pressure signal, M_{ou} = 1.344 and f = 300 Hz.

and another upstream-propagating shock was analyzed and found to predict weak reflections in unlike-sense. Therefore the strong reflection must arise from the entire shock/boundary-layer interaction region. The explanation probably includes two-dimensional effects, such as the variation of the local effective areas caused by rapid growth of the displacement thickness, but it also may include other factors not currently recognized.

4.3 Summary and Comments on Results

Detailed measurements of shock-position histories and fluctuating pressure distributions were made in a moderate-area-ratio, two-dimensional diffuser for the shock Mach numbers of 1.1 to 1.35. Data were taken with and without excitation near the downstream end.

In the absence of excitation, the shock-position spectra displayed two peaks for attached flow and one peak for separated flow conditions. These natural frequencies varied strongly as functions of shock strength. Pressure fluctuation amplitudes were generally less than 2% of the local static pressure throughout the diffuser.

Small-amplitude, periodic oscillations were generated by modulating the cross-sectional area near the diffuser end at frequencies up to 330 Hz. The resultant shock displacement and static-pressure-amplitude/phase-angle patterns suggest that at least some of the significant aspects of the diffuser response can be described by relatively simple acoustic wave concepts. It is necessary to include the streamwise variation of the flow speed, and application of the proper boundary conditions at the shock is imperative.

The character of the wave reflection process at the shock (i.e., the acoustic impedance) was found to depend strongly on the shock strength, contrary to expectations based on the known interaction characteristics of planar shocks and pressure waves. It appears that the reflection process depends on the entire shock/boundary-layer interaction region in a manner not currently understood.

Since knowledge of the proper boundary conditions at the shock is necessary for predicting diffuser response, understanding the wave reflection process at the shock emerges from this study as an important and possibly key problem.

An extensive data base was compiled whose detailed analysis is beyond the scope of this experimental effort. Such analysis offers the potential of improving our capability to predict the diffuser response substantially beyond the current level. The data also are applicable to the verification of theoretical prediction methods.

5. PUBLICATIONS

Results obtained in the first phase of the contract were documented in the following paper:

* M. Sajben and J. C. Kroutil, Effects of Approach Boundary-Layer Thickness on Oscillating, Transonic Diffuser Flows Including a Shock, AIAA Paper No. 80-0347, presented at the AIAA 18th Aerospace Sciences Mtg., Pasadena, CA, 14-16 January 1980. The paper is being revised for publication in the AIAA Journal.

The volume of the data obtained in the second phase of the contract makes it mandatory to publish the results in at least two papers. The first of these is being prepared for submittal to the AIAA Journal:

* M. Sajben, T. J. Bogar, and J. C. Kroutil, The Response of a Transonic Diffuser Flow to Perturbations Imposed at the Downstream End.

A second paper is also planned for the AIAA Journal:

* M. Sajben and T. J. Bogar, On the Mechanisms Responsible for Self-Excited Oscillations in Diffuser Flows Including a Shock.

6. PROFESSIONAL PERSONNEL

- Miklos Sajben, Senior Scientist
- Thomas J. Bogar, Research Scientist
- Joseph C. Kroutil, Lead Engineer - Design

7. INTERACTIONS

The experience and understanding gained from this work enabled M. Sajben to provide useful consultation to McDonnell Douglas Astronautics Company on a specific project (AIAAM missile) and also related to technology development.

These contacts gave clear indications that the information obtained in this contract is of immediate and direct interest for the development of ramjet propulsion systems for tactical missile applications. This recognition led to active participation by MDRL in a Workshop for Ramjet Pressure Oscillations, held 7-9 September 1979 in Monterey, CA, as part of the 1979 JANNAF Propulsion Conference. The workshop, organized by Professor F. E. C. Culick of the California Institute of Technology on behalf of AFAPL, was attended by approximately 40 invited participants from government, industry and academe.

At the workshop, contact was made with representatives from the Naval Weapons Center (NWC, China Lake). The interest expressed by Mr. Patrick J. Hall (reporting to J. Mahoney, Airbreathing Propulsion Division) prompted a visit by M. Sajben to NWC on September 1979 for a detailed presentation and technical discussions, followed by the submittal of an unsolicited MDRL proposal to NWC for a two-year study of forced oscillations in two-dimensional diffusers. This proposal differed from the current contract in several important respects: the throat is supersonic, the shock strengths to be investigated range up to a Mach number of 2.2, and the oscillation amplitudes are large (15%). This proposal was endorsed by NWC to the Office of Naval Research (ONR), and funding for one year was awarded to start on 1 July 1980.

Another valuable contact established at the Monterey workshop was Mr. Thomas Rogers of the Marquardt Company. Mr. Rogers has extensive engineering experience with the pressure oscillation problem; his comments, ideas and advice proved to be most helpful.

Considerable interest in this work exists at NASA-Ames Research Center (Dr. Thomas J. Coakley), primarily as an interesting test case for numerical computation methods capable of predicting separated transonic flows. This interest resulted in a presentation by Dr. Sajben at NASA-Ames Research Center on 6 September 1979.

Dr. Sajben attended the AIAA 18th Aerospace Sciences Meeting on 14-16 January 1980 in Pasadena, CA. Numerous conversations were held with people interested in this general subject area. Dr. Wilbur Hankey (AFFDL), who has been successful in the prediction of transonic oscillatory phenomena, indicated an interest in attempting to duplicate MDRL data by numerical computations.

8. NEW DISCOVERIES

No invention disclosures were filed during the second year of this contract. The results obtained are of a scientific import with a primary purpose to assist development of predictive theories.

9. RELATED RESEARCH

The contract work is complemented by a related IRAD effort, initiated in 1976; this IRAD effort includes both experimental and theoretical contributions.

The experimental work consists of time-resolved measurements of phase-averaged streamwise velocity distributions in the diffuser used for the present contract, using a laser velocimeter. Measurements were made in the core flow, extending from the throat to the end of the divergent section. This range includes both subsonic and supersonic regions. The data agree closely with data obtained in the contract.

The theoretical effort (by Dr. Meng-Sing Liou) produced an analytical-numerical description of the shock/boundary-layer interaction for shocks of sufficient strength to cause local flow separation. The results of this analysis were incorporated in an existing unsteady diffuser flow code developed during 1978.

REFERENCES

1. M. Sajben, J. C. Kroutil and C. P. Chen, A High-Speed Schlieren Investigation of Diffuser Flows with Dynamic Distortion, AIAA Paper No. 77-875 (1977).
2. M. Sajben, J. C. Kroutil, and C. P. Chen, Unsteady Transonic Flow in a Two-Dimensional Diffuser, AGARD Conference Proceedings No. 227, Unsteady Aerodynamics (1977).
3. C. P. Chen, M. Sajben, and J. C. Kroutil, Shock Wave Oscillation in a Transonic Diffuser Flow, AIAA J. 17, 1076 (1979).
4. M. Sajben and J. C. Kroutil, Unsteady Transonic Flows in a Two-Dimensional Diffuser, Annual Technical Report, AFSOR-TR-78-1277 (31 May 1978).

5. M. Sajben and J. C. Kroutil, Effects of Approach Boundary Layer Thickness on Oscillating, Transonic Diffuser Flows Including a Shock, AIAA Paper No. 80-0347, AIAA 18th Aerospace Sciences Meeting, Pasadena, CA, 14-16 Jan 1980.
6. M. S. Liou and M. Sajben, Analysis of Unsteady Viscous Transonic Flow with a Shock Wave in a Two-Dimensional Channel, AIAA Paper No. 80-0195 (1980).
7. M. Sajben and R. C. Crites, Real-Time Optical Measurement of Time-Dependent Shock Position, AIAA J. 17, 910 (1979).
8. M. Sajben and J. C. Kroutil, Unsteady Transonic Flows in a Two-Dimensional Diffuser, Annual Technical Report, AFOSR-TR-79-0990 (31 May 1979).

APPENDIX A: NOMENCLATURE

Symbols

f	frequency
h	channel height
M	Mach number
p	pressure
S	power spectral density
t	time
x	streamwise coordinate (x = 0 at throat, positive streamwise)
y	vertical coordinate (y = 0 on bottom wall)
ϕ	phase angle

Subscripts

x-location references:

o	plenum
*	throat
e	exit
σ	shock

y-location references:

m	midstream (for $\tilde{y}$ = 0.432, core probe or line scan system height)
u	upper wall

other

s	static
t	total

Supercripts

$\bar{(\ )}$	time-mean component
$(\ )'$	time-dependent component
$\hat{(\ )}$	rms of time dependent component
$\tilde{(\ )}$	normalized by throat height ($=h_*$)

Subscripts and superscripts may appear in combination.

END

DATE
FILMED
9-80

DTIC